3964 J. Med. Chem. 2010, 53, 3964–3972
DOI: 10.1021/jm901805m

Journal of Medicinal Chemistry Article

Phenylcinnamides as Novel Antimitotic Agents

Benjamin J. Leslie, Clinton R. Holaday, Tran Nguyen, and Paul J. Hergenrother*

Roger Adams Laboratory, Department of Chemistry, University of Illinois at Urbana—Champaign, 600 S. Mathews Avenue, Urbana, Illinois 61801

Received December 5, 2009

Compound **8H** is a phenylcinnamide that induces G2/M-phase cell cycle arrest and cell death in cancer cell lines. Here we show that **8H** exerts its cytotoxic activity through disruption of microtubule dynamics in vitro and in cell culture. A series of cinnamide derivatives were synthesized and evaluated, and several new compounds were identified that improve on the activity of the parent compound, with IC_{50} values for induction of cell death ranging from 1 to 10 μM. Notably, these compounds retain potency in the HL-60/VCR leukemia cell line, which is resistant to antimitotic cancer drugs vincrisitine and paclitaxel through up-regulation of P-glycoprotein drug efflux pumps. As P-glycoprotein expression is often responsible for drug resistance in cancer and the exclusion of compounds from the central nervous system, **8H** and its derivatives merit further examination as potential antimitotic therapeutics, specifically for brain cancers and cancers that are resistant to standard antimitotic agents.

Introduction

Microtubules are large, dynamic copolymers comprised of alternating α- and β-tubulin subunits that form long, tubular, rodlike structures inside eukaryotic cells. Their highly ordered structures, rigidity, and their ability to grow and shrink via polymerization/depolymerization mechanisms are critical to their function in several cellular processes, including the maintenance of cell shape, motility, and cell signaling.[1] Perhaps the most important role of microtubules is during mitosis, where they serve to organize and segregate chromosomes.

Several classes of small molecules are known that perturb microtubule dynamics (and thus mitosis) by binding tubulin or microtubules (Figure 1). Compounds that inhibit tubulin polymerization and destabilize microtubules include colchicine (**1**), the combretastatins (**2**), the cryptophycins, estramustine, the halichondrins, nocodazole and the *Vinca* alkaloids (**3**, **4**). Compounds that stabilize microtubules include discodermolide, eleutherobins, the epothilones, laulimalide, the sarcodictyins, and the taxanes (**5**).[1−3] Both microtubule stabilizers and destabilizers alter the tubulin−microtuble equilibrium causing mitotic arrest and ultimately apoptotic cell death. Because of the clinical success of microtubule-affecting compounds such as paclitaxel, the *Vinca* alkaloids, and epothilone derivatives in the treatment of a wide variety of cancers, it has been argued that microtubules represent the single most important protein target for anticancer therapy.[3−5]

These antimitotic drugs, however, are not without limitations. Many, including paclitaxel (**5**) and the *Vinca* alkaloids (**3** and **4**), are large (MW > 700 Da) natural products that display ADME-Tox[a] shortcomings (including poor water solubility, bioavailability, and significant dose-limiting toxicity). In addition, these large natural products are substrates for the P-glycoprotein (P-gp) drug efflux pump, and multidrug resistance (MDR) after drug exposure is a common problem observed with this class of compounds.[2,6−9] Furthermore, drugs such as taxanes are typically poor chemotherapeutics for the treatment of many brain cancers, as high levels of P-gp in the blood−brain barrier (BBB) and the chemical properties of the molecules themselves prevent significant accumulation of drug in the brain. Because of these factors, there has been an intense search for more effective antimitotics.[1,2,5,8,10−16]

We report herein the characterization of a novel anticancer compound, **8H**, and its derivatives, which cause cell death through destabilization of microtubules. These low molecular weight compounds are readily synthesized, show efficacy in cell lines resistant to conventional antimitotics, and are predicted to have increased blood−brain barrier (BBB) permeability relative to many clinically used antimitotics.

Results

We have previously reported the discovery of compound **8H** (Figure 1), a small molecule that induces cell death in cancer cell lines at low micromolar concentrations.[17] Structural features of **8H**, including the trimethoxyphenyl moiety (found in colchicine, combretastatin A-4, and several synthetic derivatives), suggested that **8H** exerted cytotoxic action through microtubule binding and mitotic arrest. Given the documented need for antimitotics that are not substrates for P-gp drug efflux, our goal was to determine the mechanism of **8H**-induced cell death, to elucidate structure−activity

*To whom correspondence should be addressed. Phone: 1-217-333-0363. Fax: 1-217-244-8024. E-mail: hergenro@illinois.edu.

[a] Abbreviations: ADME-Tox, absorption, distribution, metabolism, excretion, and toxicity; BBB, blood−brain barrier; CNS, central nervous system; DIPEA, diisopropylethylamine; DMAP, 4-(dimethylamino)pyridine; DMSO, dimethyl sulfoxide; EGTA, ethylene glycol tetraacetic acid; FBS, fetal bovine serum; HATU, 2-(1*H*-7-azabenzotriazol-1-yl)-1,1,3,3-tetramethyluronium hexafluorophosphate; IC_{50}, half maximal inhibitory concentration; IgG, immunoglobulin G; M-phase, metaphase; MDR, multidrug resistant; MeOH, methanol; MTS, 3-(4,5-dimethylthiazol-2-yl)-5-(3-carboxymethoxyphenyl)-2-(4-sulfophenyl)-2*H*-tetrazolium, inner salt; P-gp, P-glycoprotein; PBS, phosphate-buffered saline; PI, propidium iodide; PIPES, piperazine-1,4-bis(2-ethanesulfonic acid); SAR, structure−activity relationship.

 Published on Web 04/22/2010

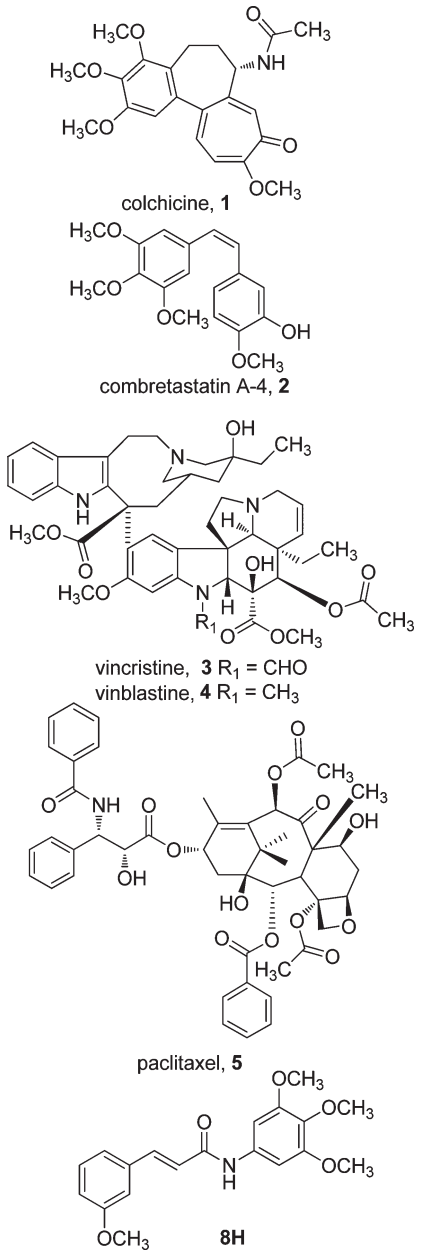

Figure 1. Structures of selected antimitotic compounds.

relationships, and to create more potent versions that would be suitable for in vivo evaluation.

8H-Induced Cell Death Is Preceded by M-Phase Arrest. Flow cytometric analysis of DNA content in **8H**-treated cells shows that this compound arrests cells in either the G2- or M-phase of the cell cycle in a dose-dependent manner.[17] To determine if **8H** induces arrest in the M-phase of the cell cycle, we used an antibody specific for Ser10 phosphorylation of histone H3, a common mitotic marker.[18,19] Double thymidine-blocked G1/S-arrested HeLa cells were released by washing two times in fresh media and grown in fresh media in the presence of 25 μM **8H**, 100 nM **1**, or an equal volume of DMSO vehicle (Figure 2). After 9 h, cells were fixed in 3% formaldehyde−PBS, permeabilized with 90% MeOH, treated with a mouse antibody raised against phospho(Ser10) histone H3, followed by an Alexa-Fluor 488-conjugated goat antimouse 2° antibody. Cells were then briefly treated with propidium iodide (PI) to stain

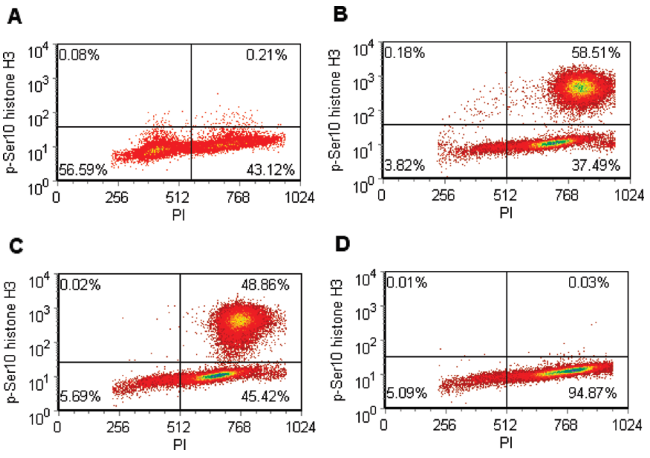

Figure 2. Cell cycle analysis of synchronized HeLa cells treated for 9 h with **8H**, colchicine, or vehicle. Double thymidine-blocked cells were released by washing two times in fresh media and plated in fresh media with compound or vehicle. After 9 h, cells were fixed in 3% formaldehyde−PBS, permeabilized in 90% MeOH, treated with a primary antibody raised against phospho(Ser10) histone H3, a mitosis-specific cellular marker, and a green fluorescent 2° antibody, and propidium iodide (PI). (A−D), Alexa-Fluor 488 2° antibody-conjugate fluorescence intensity vs propidium iodide fluorescence intensity. (A) Vehicle control shows primarily G1-arrested cells (bottom left quadrant), with no M-phase cells (top right quadrant). (B) Colchicine (100 nM) produces strong G2/M arrest (right quadrants), with 59% of cells in M-phase. (C) Compound **8H** (25 μM) produces strong G2/M arrest (right quadrants), with 49% of cells in M-phase. (D) M-Phase fluorescence staining is specific for cells containing Ser10 phosphorylation on histone H3, as cells treated with 25 μM **8H** but stained with PI and 2° Ab only (no primary Ab) show strong G2/M arrest (bottom right quadrant) and low 2° Ab background (top quadrants).

DNA, washed with PBS, and analyzed in a dual-laser flow cytometer. In this experiment the G2/M population was positive by PI staining (upper and lower right quadrants), and M-phase arrested cells were further distinguished from G2-arrested cells through staining with an antibody to phospho(Ser10) histone H3. Cells arrested in mitosis exhibited intense fluorescence staining in both the PI channel (G2/M population) and the AF-488 channel (M-phase cells), the upper right quadrant of the graphs in Figure 2.

After 9 h of treatment with DMSO vehicle, 57% of the cell population had returned to the G1 phase (bottom left quadrant), and less than 1% of the cell population was in M-phase (top right quadrant, Figure 2A). Treatment with colchicine caused 59% of the cell population to arrest in metaphase (top right quadrant), with all but 4% of the remaining population halted in G2 (Figure 2B). Similarly, a 9 h treatment with **8H** caused significant G2/M arrest as assessed by propidium iodide staining, with 49% of the cell population staining positive for histone H3 Ser10 phosphorylation, meaning that **8H**, like colchicine (**1**), arrests cells in mitosis (Figure 2C). Similar results for **8H** and control compounds were obtained in U-937 (human lymphoma) cells, indicating that mitotic arrest is not limited to a specific cell line (data not shown). M-Phase fluorescence staining is specific for cells containing Ser10 phosphorylation on histone H3, as cells treated with 25 μM **8H** but stained with PI and 2° antibody only (no primary Ab) show strong G2/M arrest in the PI channel (bottom right quadrant) but no staining in the AF-488 channel (top quadrants) (Figure 2D).

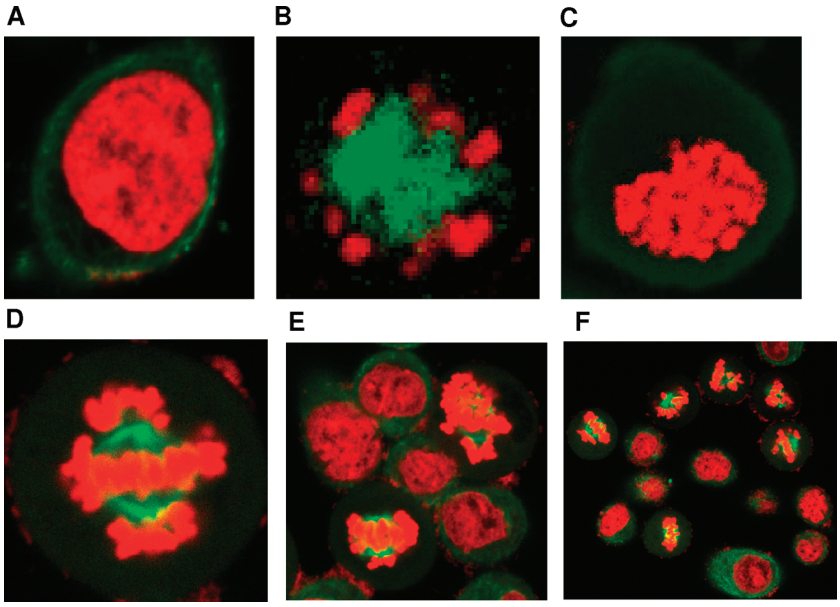

Figure 3. Effects of **8H** on microtubule dynamics in vivo. (A−E) Representative microscopic images of HeLa cells treated with (A) DMSO, (B) 10 nM paclitaxel, (C) 100 nM colchicine, and (D−F) 25 μM **8H** for 6 h. Note the stray chromosomes that have not progressed to the metaphase plate in the **8H**-treated cells. Chromosomes are stained with propidium iodide (red), and microtubules were visualized with mouse anti-α-tubulin, FITC conjugate (green). All cells are roughly 15 μm in diameter.

8H Induces Mitotic Arrest in HeLa Cells As Assessed by Microscopy. As another means of assessing the degree of M-phase arrest induced by **8H**, cells were treated with compound or vehicle control, the DNA and microtubules were stained, and cells were imaged using fluorescence confocal microscopy. For this experiment HeLa cells were allowed to adhere to acid-washed glass coverslips and then treated for 6 h with compound or DMSO vehicle. Next, the cells were washed, fixed in formaldehyde, and treated with an indirect immunofluorescent stain for microtubules in conjunction with PI staining to visualize DNA. Widefield images were obtained for DMSO- and **8H**-treated slides and manually scored for mitotic index based on DNA staining. Roughly 2000 cells were analyzed each for DMSO and **8H** treatment over three identical experiments performed on different days with different cell preparations. A paired *t* test was performed to determine if treatment of unsynchronized HeLa cells with **8H** caused a statistically significant increase in the number of mitotic cells observed compared to DMSO treatment. Mitotic index increase from 2.2% in DMSO-treated cells (SD = 1.1%, N = 3 with ~2000 cells counted each time) to 18.2% in cells treated with **8H** (SD = 4.0%, N = 3 with ~2000 cells counted each time) was highly statistically significant ($t(4) = 6.80$, two-tail $p = 0.002$). These data, when combined with the results described in Figure 2, convincingly demonstrate that **8H** treatment induces M-phase arrest in cancer cells.

8H Induces Mitotic Arrest in HeLa Cells through Disruption of Microtubule Dynamics. We next tested whether **8H** could directly affect microtubule dynamics in living cells. High-resolution images of cells treated with DMSO (Figure 3A), 10 nM paclitaxel (Figure 3B), 100 nM colchicine (Figure 3C), and 25 μM **8H** (Figure 3D−F) were obtained on a fluorescence confocal microscope. Vehicle-treated cells were observed to be predominantly in interphase, characterized by diffuse cytoplasmic tubulin staining and diffuse staining of uncondensed DNA (Figure 3A). However, treatment with **8H** produced a large increase in the amount of mitotic cells, evidenced by nuclear tubulin staining and chromosomal condensation (Figure 3D−F). The irregularity of the mitotic cells observed, as evidenced by stray chromosomes not aligned at the metaphase plate, suggests that **8H** treatment arrests cells in mitosis by affecting microtubule dynamics.[1]

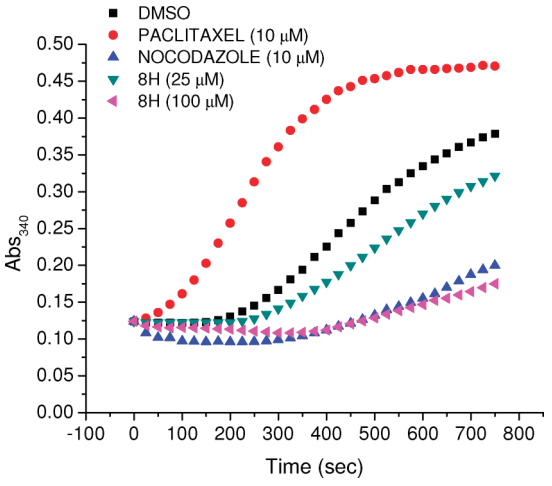

Figure 4. Effects of **8H** on microtubule dynamics. Polymerization of tubulin at 37 °C in the presence of paclitaxel (10 μM), nocodazole (10 μM), or **8H** (25 and 100 μM) was monitored continuously by recording the absorbance at 340 nm over 13 min. Data shown are representative of three independent experiments.

8H Destabilizes Tubulin Polymerization in Vitro. Although several new targets have emerged, most M-phase arresting compounds target tubulin and/or microtubules.[1,20−23] We monitored the spontaneous polymerization of bovine brain tubulin in the presence of **8H** in vitro in order to determine if the antimitotic properties of **8H** were due to direct interference with microtubule dynamics and whether this effect was due to the stabilization or destabilization of microtubule polymerization (Figure 4). In vitro, microtubule polymerization can be quantitated spectrophotometrically

Scheme 1[a]

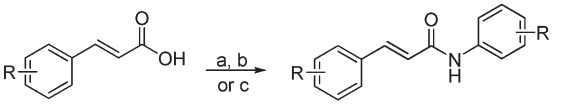

Compounds **6** - **33**

[a] Reagents and reaction conditions: (a) $(COCl)_2$, DMF, anhydrous CH_2Cl_2, room temp, 12 h; (b) $(R_5-R_9)PhNH_2$, Hünig's base, anhydrous MeCN, DMAP, microwave, 150 °C, 1.5 h ; (c) $(R_5-R_9)PhNH_2$, Hünig's base, HATU, microwave, 150 °C, 1.5 h.

as an increase in turbidity at 340 nm.[24] DMSO vehicle is known to slightly stabilize microtubules and produces an intermediate polymerization phenotype.[24] As expected, the microtubule stabilizer paclitaxel induces a strong increase in turbidity, whereas nocodazole destabilizes growing microtubules such that depolymerization at the (−)-end is faster than polymerization at the (+)-end, giving rise to a net "depolymerization" phenotype and no rise in turbidity (Figure 4).[1] Attempted polymerization of tubulin in the presence of **8H** produced a depolymerization phenotype, suggesting that **8H** and related phenylcinnamides may exert cytoxicity through destabilization of microtubule polymerization. This effect was maximal at 100 μM, while at 25 μM an intermediate effect was observed. The 100 μM concentration of **8H** used in this experiment is approximately 1 order of magnitude higher than its IC_{50} in cell culture (Tables 2 and 3); however, paclitaxel and nocodazole are routinely used at concentrations 10^3 times their IC_{50} in cell culture for optimal results in these in vitro tubulin polymerization experiments.[12,13,15]

Structure−Activity Relationship and Cytotoxicity of Derivatives of 8H. In an effort to define a structure−activity relationship (SAR) for **8H** and to identify more potent versions, several derivatives of this compound were synthesized and evaluated. Specifically, compounds that had differential substitutions on the two phenyl rings were created, as was one in which the backbone unsaturation was removed. The general synthetic route to the new derivatives of **8H** is depicted in Scheme 1, and the structures of new derivatives are shown in Table 1. Amidation was accomplished either by treatment of the corresponding acid with oxalyl chloride and catalytic *N*,*N*-dimethylformamide in CH_2Cl_2 followed by DMAP-promoted amidation via microwave irradiation at elevated temperature and pressure or via direct amidation of the acid in the presence of HATU and DIPEA to provide phenylcinnamides **6**−**33** in modest yields after automated purification on a normal-phase medium pressure liquid chromatography system. Increasing reaction temperature led to increased percentages of conjugate-addition side products, whereas decreasing reaction temperature resulted in decreased product yield.

All compounds were assessed for their ability to induce death in two human cancer cell lines: U-937 (human lymphoma) and HeLa (human cervical cancer) using either the MTS bioreduction assay (Promega) or sulforhodamine B biomass assay[25] (Table 2). Toxicity of each compound was typically assessed three times on different days, and IC_{50} data are reported as the average ± SD. Compound **8H** induces death in the U-937 and HeLa cell lines with IC_{50} values of 3.0 ± 1.2 and 11.3 ± 2.3 μM, respectively. The derivatives lacking the olefin (compounds **31** and **32**) are largely devoid of cell death inducing properties, possibly suggesting a mechanistic role of **8H** as an electrophile, as has been seen for other antimitotics.[26,27] Removal of the methoxy group from R2 results in compounds (**8**, **9**) with greatly diminished activity. Likewise, compounds that have alterations to the 3,4,5-trimethoxy motif (**23**−**30**) also have reduced activity. Compounds lacking substitution at R7 showed a complete lack of activity (**23**−**25**, **27**, **29**, **30**), whereas substitution on R7 alone provided compounds of intermediate potency (**26**, **28**). The entire phenylcinnamide core structure of **8H** was required for activity, as neither compound **34** nor **35** showed anticancer activity.

In contrast, structural and chemical modifications to the part of the molecule derived from the carboxylic acid (**8**−**22**) produced a few derivatives that retained or surpassed the potency of **8H**. In particular, compounds with substitution at R1 (**16**) and larger groups at R2 (**20**−**22**) still induce cell death. Overall, the most active compounds (**8H**, **6**, **16**, **20**−**22**) contained the 3,4,5-trimethoxy substitution derived from the aniline building block, with ortho- or meta-substitution on the cinnamic acid side of the molecule, with increasing bulk in the meta-position leading to the most potent compounds (**20**−**22**).

Predicted Blood−Brain Barrier Penetration. The general hydrophilicity and large polar surface areas of several classes of antimitotics contributes to their poor penetration of the blood−brain barrier (BBB).[28] As the number of compounds for which experimental data on BBB penetration are publically available is extremely small, computational methods have been developed to predict a molecule's ability to enter the central nervous system (CNS). Many compounds that penetrate the blood−brain barrier (BBB) share common features: their calculated partition coefficient octanol/water ($C_{log}P$) values are typically between 1 and 3, and their predicted topological polar surface area (TPSA) is usually less than 90 Å^2.[29] Values for $C_{log}P$ and TPSA were calculated using ClogP[29] and TPSA[30] algorithms. These two values were substituted into eq 1 to calculate log BB, the predicted partition coefficient between the brain and the blood.

$$\log BB = (-0.0148\,TPSA) + (0.152\,C_{log}P) + 0.139 \quad (1)$$

Compounds with predicted values of log BB less than −0.3 are not considered capable of crossing the BBB, while values greater than zero are predicative of concentration in the brain higher than in the blood.[29,31] As shown in Table 3, the antimitotic colchicine is not predicted to cross the BBB. In contrast, the most potent **8H** derivative (compound **22**) is predicted to be brain-permeant, with a log BB value of −0.12 (Table 3).[6] These values are comparable to those of 2-methoxyestradiol, an antimitotic compound currently being investigated for treatment of CNS cancers (Table 3).[32−36]

8H and Its Derivatives Are Not Substrates of P-Glycoprotein (P-gp). In addition to the physical barriers to entry into the CNS, drug efflux pumps such as P-glycoprotein actively exclude drugs from the brain. In addition to complicating treatments of cancers of the CNS, up-regulation of these same proteins has also been observed in drug-resistant cancers from several other cell types.[37] We tested the cytotoxicity of **8H** derivatives in the HL-60 (human leukemia) cell line, as well as in HL-60/VCR, a daughter cell line that is resistant to vincrisitine and colchicine by virtue of P-gp up-regulation.[38,39] Colchicine (**1**) is a potent cytotoxin in HL-60 cells, with an IC_{50} value of 53 nM (Table 3). As **1** is a known substrate of P-gp, we found the HL-60/VCR cell line to be extremely resistant to **1**, with IC_{50} values greater

Table 1. Structures and Isolated Yields of Cinnamides **6**−**35**

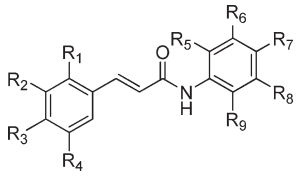

cmpd	R_1	R_2	R_3	R_4	R_5	R_6	R_7	R_8	R_9	Yield (%)
8H	H	OCH_3	H	H	H	OCH_3	OCH_3	OCH_3	H	63
6	H	OCF_3	H	H	H	OCH_3	OCH_3	OCH_3	H	60
7	H	OCF_3	H	H	OCH_3	H	H	H	H	51
8	H	OH	H	H	H	OCH_3	OCH_3	OCH_3	H	43
9	H	H	H	H	H	OCH_3	OCH_3	OCH_3	H	77
10	H	OCH_3	OCH_3	OCH_3	H	OCH_3	OCH_3	OCH_3	H	58
11	H	OCH_3	OCH_3	OCH_3	H	OCH_3	H	OCH_3	H	19
12	H	OCH_3	OCH_3	OCH_3	H	OCH_3	H	H	H	58
13	H	OCH_3	OCH_3	OCH_3	OCH_3	H	H	H	H	20
14	H	OCH_3	OCH_3	OCH_3	H	H	H	H	H	16
15	H	OCH_3	OCH_3	OCH_3	H	H	OCH_3	H	H	10
16	OCH_3	H	H	H	H	OCH_3	OCH_3	OCH_3	H	88
17	OCH_3	H	H	H	OCH_3	H	H	H	H	34
18	H	H	OH	H	H	OCH_3	OCH_3	OCH_3	H	15
19	H	H	OH	H	H	OCH_3	H	OCH_3	H	17
20	H	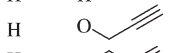	H	H	H	OCH_3	OCH_3	OCH_3	H	70
21	H	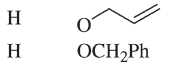	H	H	H	OCH_3	OCH_3	OCH_3	H	76
22	H	OCH_2Ph	H	H	H	OCH_3	OCH_3	OCH_3	H	60
23	H	OCH_3	H	H	H	OCH_3	H	OCH_3	H	21
24	H	OCH_3	H	H	OCH_3	H	H	H	H	44
25	H	OCH_3	H	H	H	OCH_3	H	H	H	39
26	H	OCH_3	H	H	H	H	OCH_3	H	H	85
27	H	OCH_3	H	H	H	H	H	H	H	33
28	H	OCH_3	H	H	H	$-OCH_2CH_2O-$		H	H	30
29	H	OCH_3	H	H	H	CH_3	H	CH_3	H	45
30	H	OCH_3	H	H	CH_3	H	H	H	CH_3	39
31	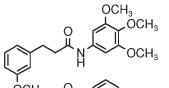									45
32	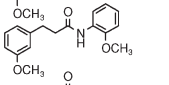									44
33	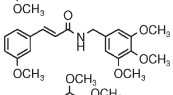									54
34	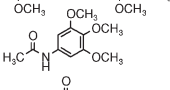									99
35	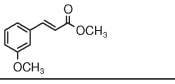									99

than 100 μM. The extreme difference in the sensitivity of these two cell lines gives resistant:sensitive (R:S) IC_{50} ratios greater than 1000:1; i.e., **1** is significantly less cytotoxic in the HL-60/VCR cell line presumably because P-gp efflux prevents it from reaching threshold concentrations inside the cell needed to produce microtubule disregulation. In contrast, compounds **8H**, **6**, and **22** retain almost full potency in the HL-60/VCR cells compared to the parent HL-60 cell line (R:S ratios of 0.98 to 3.74), indicating that these compounds are not substrates of P-glycoprotein drug transporters (Table 3).

Compound 22 Induces M-Phase Arrest. Compound **22**, the most potent compound in its class in all cell lines tested, retains almost full activity in the HL-60/VCR cell line, with an IC_{50} of 5.5 μM, indicating that it is not a substrate of P-gp (Table 3). This value is comparable to that of 2-methoxyestradiol, a compound that binds to the colchicine domain of tubulin; this compound is currently in phase I and phase II clinical trials for the treatment of multiple myeloma, glioblastoma, multiforme carcinoid, prostate, and breast cancers.[40] Like the parent **8H**, compound **22** causes microtubule disruption in cell culture (Figure 5). Given that **22** is readily

Table 2. Inhibition of Growth of U-937 (Lymphoma) and HeLa (Cervical) Human Cancer Cell Lines

compd	U-937[a,c] $IC_{50} \pm SD$ (μM)	HeLa[b,c] $IC_{50} \pm SD$ (μM)
8H	3.0 ± 1.2	11.3 ± 2.3
6	13.2 ± 7.5	4.4 ± 1.2
7	40.4 ± 9.1	9.8 ± 7.5
8	56.7 ± 1.3	18.7 ± 8.0
9	45.0 ± 7.1	> 50
10	15.3 ± 2.5	> 50
11	9.7 ± 4.8	38.9 ± 21.9
12	> 50	ND
13	> 50	> 50
14	> 50	> 50
15	22.4 ± 22.4	> 50
16	5.1 ± 0.4	6.1 ± 1.34
17	> 50	36.1 ± 6.2
18	32.0 ± 13.3	> 50
19	> 50	> 50
20	6.0 ± 1.4	2.0 ± 1.7
21	13.3 ± 0.1	5.4 ± 1.2
22	1.8 ± 0.8	2.1 ± 1.4
23	> 50	ND
24	> 50	ND
25	> 50	> 50
26	18.1 ± 6.8	ND
27	> 50	> 50
28	15.9 ± 3.5	20.1 ± 7.0
29	> 50	ND
30	> 50	> 50
31	ND	> 50
32	> 50	> 50
33	> 50	> 50
34	> 50	> 50
35	> 50	> 50

[a] Cytotoxicity in human U-937 (lymphoma) cells as assessed by MTS assay. [b] Cytotoxicity in human HeLa (cervical cancer) cells as assessed by SRB assay. [c] Error equals standard deviation of the mean from at least three separate experiments. Values without SD represent the average of two IC_{50} values generated on separate days. ND = not determined.

Table 3. Inhibition of Growth HL-60 and HL-60/VCR (Leukemia) Human Cancer Cell Lines

cmpd	Predicted $C_{log}P$[a]	Predicted $_{log}BB$[a]	HL-60[b] $IC_{50} \pm SD$ (μM)	HL-60/VCR[b] $IC_{50} \pm SD$ (μM)	Selectivity R/S[c]
8H 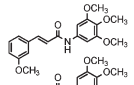	2.9	-0.39	3.1 ± 2.3	11.6 ± 3.8	3.74
6 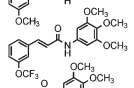	4.1	-0.22	13.2 ± 5.6	13.1 ± 8.4	0.99
22 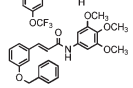	4.7	-0.12	5.6 ± 2.3	5.5 ± 1.7	0.98
colchicine (**1**)	1.2	-0.91	0.053 ± 0.06	>100	>1000
2-methoxyestradiol	3.6	-0.04	3.4 ± 5.0	0.90 ± 0.10	0.26

[a] Predicted $C_{log}P$ and log BB values for all compounds calculated using ClogP and TPSA algorithms (see text). [b] Cytotoxicity in human HL-60 and HL-60/VCR (leukemia) cells as assessed by MTS assay. Error equals standard deviation of the mean from at least three separate experiments. Values without SD represent the average of two IC_{50} values generated on separate days. [c] Ratio of toxicity in resistant HL-60/VCR to sensitive HL-60 cell line.

synthesized via O-alkylation of compound **8**, we envision this as a lead pharmacophore for future molecule development.

Discussion

Antimitotics are an especially important class of anticancer agents, and there is a great need for compounds that are easily synthesized and that possess improved properties (solubility, stability, toxicity, brain permeability) over those of natural products. We have therefore synthesized a small library of derivatives of lead molecule **8H** via convenient one- or two-step protocols to provide useful quantities of compounds (10−100 mg) in modest yields. We have shown that **8H** and its phenylcinnamide derivatives induce M-phase cell cycle arrest leading to cell death and cause disruption of microtubule dynamics in vitro and in cell culture. On the basis of its structural similarity to colchicine and combretastatin A-4, we hypothesize that tubulin is the primary molecular target of **8H** and its derivatives, causing cell cycle arrest through destabilization of microtubule assembly, similar to a "depolymerizer" compound such as colchicine or vincristine.

One major limitation of antimitotic drugs such as vincristine and paclitaxel is that they are substrates of P-gp efflux pumps and thus are actively excluded from cell lines that express P-gp, where it acts to excrete xenobiotics.[41] Therefore, cell types that natively express P-gp, such as epithelial cells of the gastrointestinal tract, liver, kidneys, and the capillaries of the brain and gonads, are innately resistant to some degree. Furthermore the presence of mdr-1 gene transcripts (which code for P-gp) have been observed in 39 of the 60 cell lines that comprise the NCI-60 panel of cancer cell lines, and a strong correlation exists between its expression level and cellular resistance to several chemical therapeutics.[42] Thus, our finding that several compounds containing the phenylcinnamide core retain potency in the HL-60/VCR cell line, a model cell line for multidrug resistant cancers, is significant. The fact that **8H** and its derivatives do not appear to be substrates of the P-gp efflux pump, coupled with the fact that calculated log BB values predict increased brain permeability over several natural product antimitotics, makes this an exciting new class of anticancer compounds.

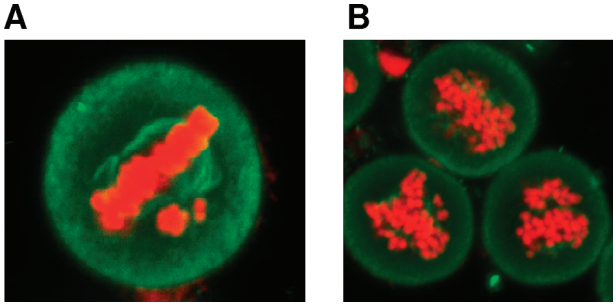

Figure 5. Effects of **22** on microtubule dynamics in vivo. (A, B) Representative microscopic images of HeLa cells treated with 25 μM **22** for 6 h, showing metaphase cells with misaligned chromosomes (A) and mitotic cells lacking microtubule structures (B). Chromosomes are stained with propidium iodide (red), and microtubules were visualized with mouse anti-α-tubulin, FITC conjugate (green). All cells are roughly 15 μm in diameter.

Materials and Methods

Chemistry. Unless otherwise stated chemical reagents were purchased from Sigma-Aldrich and used without further purification. Solvents (HPLC grade, no inhibitors) were passed through activated alumina in an Integrated Technologies solvent drying system under UHP N_2. All NMR experiments were recorded on Varian Unity 400 and 500 MHz spectrometers with residual undeuterated solvent as an internal reference. The following data are reported: chemical shift (ppm), coupling constant J (Hz), multiplicity (s = singlet, d = doublet, t = triplet, q = quintet, m = multiplet), and integration. High-resolution mass spectral data

were recorded on Micromass Q-TOF Ultima hybrid quadrupole/time-of-flight (ESI+) and Micromass 70-VSE (EI) mass spectrometers at the University of Illinois Mass Spectrometry Laboratory. Thin layer chromatography was visualized by UV or stained with cerium ammonium molybdate (CAM), ninhydrin, or DPIP (0.5 mg/mL 2,6-dichloroindophenolate hydrate in EtOH). Flash chromatography was performed on EMD Biosciences silica gel 60 (230−400 mesh) using reagent-grade solvents. All new chemical entities were analyzed for purity on Rainin Dynamax SD-200 or Finnigan LCQ Deca XP HPLCs detecting eluted solute at 254 nm equipped with an Alltech Alltima analytical C18 column (20 mm × 2.1 mm × 3 μm) with an acetonitrile−0.1% trifluoroacetic acid in Millipore Milli-Q-filtered water solvent gradient. All compounds were purified to at least 95% purity before characterization and use in biological assays. In the event that a compound was not of sufficient purity after flash chromatography, the compound was repurified via preparatory HPLC on a Rainin Dynamax SD-200 fitted with a Vydac 218TP1022 (250 mm × 22 mm × 5 μm) C18 column.

Biological Materials. Purified bovine brain tubulin was a gift of Professor Tim Mitchison (Harvard Medical School). Before use, polymerization-competent tubulin was repurified following Mitchison's polymerization/depolymerization cycling protocol and quantitated spectrophotometrically using $\varepsilon_{280nm} = 115\,000\ M^{-1}\ cm^{-1}$.[43] MTS/PMS CellTiter 96 cell proliferation assay reagent was purchased from Promega (Madison, WI). Fetal bovine serum was purchased from Biomeda (Foster City, CA). FITC-conjugated mouse anti-α-tubulin antibody, sulforhodamine B sodium salt, formaldehyde (37% solution in water), glutaraldehyde (50% aqueous solution, photographic grade) were purchased from Sigma-Aldrich (St. Louis, MO). Goat antimouse IgG/Alexa-Fluor 488 conjugate and propidium iodide were from Molecular Probes (Eugene, OR). Goat serum (10% solution) was from Invitrogen (Carlsbad, CA). Vectashield mounting medium was from Vector Laboratories (Burlingame, CA). RPMI-1640 cell culture medium was obtained from the UIUC School of Chemical Sciences Cell Media Facility. Microtiter plates (96-well, tissue culture-treated), microscope slides, no. 1 microscope coverslips, Eppendorf tubes, and all other reagents were purchased from Fisher (Chicago, IL).

Cell Culture. HeLa and U-937 cell lines were purchased from American Type Culture Collection (Manassas, VA). HL-60 and HL-60/VCR cell lines were a generous gift from Professor Russell J. Mumper (University of North Carolina). For all experiments, cell lines were cultured in RPMI-1640 supplemented with 10% FBS and 1% penicillin/streptomycin in tissue-culture treated flasks and Petri dishes and maintained at 37 °C in a humidified 5% CO_2 incubator.

Flow Cytometric Analysis. HeLa cells were synchronized in G1/S following a standard double thymidine-block protocol.[44] Arrested cells were released by washing three times with thymidine-free medium and immediately harvested by trypsinization, counted using a hemocytometer, and plated (1.5×10^6 per plate) in 10 cm cell-culture-treated Petri dishes containing 12 mL of cell growth medium. Compound **8H** (25 μM), colchicine (100 nM), cycloheximide (2.5 μM), or an equal volume of DMSO vehicle was added, and cells were incubated for 9 h at 37 °C in a humidified 5% CO_2 incubator. Cells were rapidly harvested by scraping, washed with PBS, pH 7.4, and fixed for 10 min in 500 μL of PBS, pH 7.4, containing 3% formaldehyde in sealed 1.7 mL Eppendorf tubes in a 37 °C water bath. After fixation, cells were incubated on ice for 1 min and centrifuged for 5 min at 200*g*, and PBS was removed via aspiration. Cells were gently resuspended in 300 μL of MeOH by dropwise addition of ice-cold 100% MeOH to a gently vortexed tube. Cell suspensions were incubated on ice for 30 min and stored overnight at −20 °C to permeabilize cells. Permeabilized cells were then washed twice with blocking solution (0.5% BSA in PBS, pH 7.4) to remove MeOH and resuspended in 500 μL of blocking solution and incubated at 25 °C for 10 min. Blocking solution was removed by aspiration, and cells were resuspended in 100 μL of blocking solution containing mouse anti-phospho(Ser10) histone H3 antibody at 1:25 dilution and incubated for 30 min at 25 °C. A portion of the **8H**-treated cells (0.5×10^6) were separated before treatment and were incubated in blocking solution alone as a control for nonspecific 2° antibody binding. After incubation, cells were washed 3 × 1 mL in blocking solution and were resuspended in 200 μL of blocking solution containing goat antimouse IgG/Alexa-Fluor 488 conjugate (1:1000) and incubated for 30 min at 25 °C. After washing 3 × 1 mL in blocking solution, cells were resuspended in 200 μL of PBS containing 100 μg/mL RNase A and incubated for 30 min at 25 °C, at which point 100 μL of propidium iodide (1 mg/mL in PBS) was added and incubated for an additional 30 min. Cells were washed 3 × 1 mL of PBS, resuspended in 400 μL of PBS, and immediately analyzed on a BD Biosciences LSR II flow cytometer using a 488 nm excitation laser, monitoring green and red channels with 530 ± 15 and 695 ± 20 nm bandpass filters, respectively.

Assessment of Cell Viability via Sulforhodamine B Assay. Cytotoxicity of compounds against the HeLa cell line was assessed using the sulforhodamine B (SRB) assay in 96-well plate format using the optimized protocol of Vichai and Kirtikara.[25] Briefly, 2 μL of a dilution series of each compound dissolved in DMSO were added to 98 μL of appropriate growth medium at five replicates per concentration. Then cells suspended in 100 μL of growth medium at a concentration of 5×10^4 cells/mL were added, and the plate was incubated in a 5% CO_2 incubator for 72 h at 37 °C. After 72 h, media were removed from the plates and cells were fixed by addition of 100 μL of ice-cold 10% (w/v) trichloroacetic acid (TCA) in water and placed in a refrigerator. After overnight incubation, TCA was removed by washing plates four times with distilled water, and plates were allowed to dry at room temperature overnight. Sulforhodamine B, sodium salt (100 μL of 0.06% w/v solution dissolved in 1% acetic acid) was added to each well, and the plates were incubated at room temperature for 30 min, after which time unbound sulforhodamine B was removed by washing 4 times with 1% acetic acid. SRB bound to proteins was released by addition of 200 μL of 10 mM Tris, pH 10.5, and the absorbance of each well was measured at 510 nm on a Molecular Devices SpectraMax 384 Plus plate reader after 30 min of incubation at room temperature. Five replicates of each compound were added at 10 different concentrations ranging from 100 μM to 5 nM in a 96-well plate. Each plate contained internal positive (known cytotoxic compound at 100 μM) and negative (DMSO vehicle) controls for calibration of the percentage of cell death observed in each well, which were used to construct a dose−response curve and calculate an IC_{50} by fitting the data to a four-parameter logistic curve of the equation $y = (A - D)/[1 + (x/C)^B] + D$.

Assessment of Cell Viability via MTS Assay. Cytotoxicity of compounds against the U-937, HL-60, and HL-60/VCR cell lines was assessed using the MTS assay according to the manufacturer's specifications (Promega). Briefly, an amount of 2 μL of a dilution series of each compound dissolved in DMSO was added to 98 μL of appropriate growth medium at five replicates per concentration. Then cells suspended in 100 μL of growth medium at a concentration of 1×10^5 (U-937 and HL-60) or 1.5×10^5 (HL-60/VCR) cells/mL were added, and the plate was incubated in a 5% CO_2 incubator at 37 °C. After 72 h, plates were removed and processed as per the MTS protocol, wherein a 20 μL solution of MTS ((3-(4,5-dimethylthiazol-2-yl)-5-(3-carboxymethoxyphenyl)-2-(4-sulfophenyl)-2*H*-tetrazolium, inner salt) and PMS (phenazine methosulfate) in PBS was added to each well, and plates were returned to a 5% CO_2 incubator until the signal from vehicle-treated cells reached the upper end of the linear range of the assay (OD ≈ 1.5, roughly 30 min for U-937 and HL-60 cell lines, up to 2 h for HL-60/VCR cell line). Absorbance of each well was measured at 490 nm on a Molecular

Devices SpectraMax 384 Plus plate reader. Five replicates of each compound were added at 10 different concentrations ranging from 100 μM to 5 nM in a 96-well plate. Each plate contained internal positive (known cytotoxic compound at 100 μM) and negative (DMSO vehicle) controls for calibration of the percentage of cell death observed in each well, which were used to construct a dose−response curve and to calculate an IC_{50} by fitting the data to a four-parameter logistic curve of the equation $y = (A - D)/[1 + (x/C)^B] + D$.

Tubulin Polymerization Assay. Polymerization of tubulin was monitored by measuring absorbance at 340 nm in a 384-well plate Molecular Devices Spectramax 384 Plus spectrophotometer (Sunnydale, CA) preheated to 37 °C. To a 0.5 mL polypropylene tube on ice was added 40 μL of ice-cold 1.25× BRB-80 buffer (100 mM PIPES, pH 6.8, 1.25 mM $MgCl_2$, 1.25 mM EGTA, 1.25 μM GTP (added from 100 mM stock immediately before use), 6.25% v/v glycerol). To individual aliquots of buffer was also added DMSO or compound in DMSO (DMSO 0.6% final in buffer, paclitaxel, and nocodazole were used at final concentrations of 10 μM, **8H** at 25 and 100 μM). To this solution was rapidly added 10 μL of 15 mg/mL polymerization-competent tubulin in ice-cold 500 mM K-PIPES, pH 6.8, 0.5 mM $MgCl_2$, buffer, which had been thawed on ice immediately before use. Solutions were mixed rapidly on ice and then immediately transferred to a 384-well plate. Final concentrations of reagents in polymerization reaction were as follows: 80 mM PIPES, pH 6.8, 1.0 mM $MgCl_2$, 1.0 mM EGTA, 1.0 μM GTP, 5% glycerol, 0.5% DMSO, 3 mg/mL tubulin. Turbidity at 340 nm corresponding to polymerization was assessed every minute for 60 min.

Laser Fluorescence Confocal Microscopy. For laser fluorescence confocal microscopy, HeLa cells were grown on nitric acid-washed no. 1 coverslips overnight in a 5% CO_2 incubator h at 37 °C. Compound in DMSO or DMSO vehicle alone (0.2% DMSO final) was added to the cells at 40% or 70% confluency and further incubated for 6 h (70% confluent cells) or 16 h (40% confluent cells). Cells were washed briefly with BRB-80 and fixed for 10 min with 0.5% glutaraldehyde in BRB-80, then permeabilized for 15 min in 1% Triton X-100 in PBS. After washing three times in PBS, pH 8.0, unreacted aldehydes were reduced with three 7 min incubations of 1 mg/mL $NaBH_4$ dissolved in PBS, pH 8, immediately before use. Cells were given three rinses with a solution of 0.1% Triton X-100 in PBS, pH 8.0 (PBST), and blocked 20 min in 10% goat serum. FITC-conjugated anti-α-tubulin was added at a 1:100 dilution in 10% goat serum, and the cells were incubated for 1 h, then washed 3 × 10 min in PBST. Goat antimouse IgG/Alexa-Fluor 488 conjugate was diluted 1:200 in 10% goat serum and incubated with cells for 1 h, then washed three times with PBST. Cells were incubated in PBS containing 10 μg/mL propidium iodide and 1 μg/mL RNase A for 15 min, washed twice with PBS, once with H_2O, and mounted onto microscope slides using 8 μL of Vectashield mounting medium and sealed with colorless nail polish.[45] Samples were visualized immediately on a Zeiss LSM 510 laser scanning confocal microscope, 63× oil DIC objective, 1.4 NA. Wide-field images were acquired by moving the stage to 10−15 random locations on each slide, thereafter only adjusting the stage in the *z*-direction to bring a maximal number of cells into focus.

In Silico Prediction of Biological Properties. SMILES formulas for all new compounds were generated in Chemdraw (Cambridgesoft Corp., Cambridge, MA). SMILES formulas for known antimitotics were downloaded from the PubChem database.[46] Values for calculated partition coefficient octanol/water ($C_{log}P$) and topological polar surface area (TPSA) were calculated using Daylight software (Daylight Chemical Information Systems, Inc., Aliso Viejo, CA) which contains implementations of ClogP[29] (BioByte Corp., Claremont, CA) and TPSA[30] algorithms. Predicted log BB was calculated using the formula $\log BB = -0.0148\,PSA + 0.152\,C_{log}P + 0.139$.[29]

Acknowledgment. We thank Professor Russell J. Mumper (University of North Carolina) for the generous gift of HL-60 and HL-60/VCR cell lines, and Professor Timothy Mitchison (Harvard Medical School) for the generous gift of soluble bovine brain tubulin. This work was supported by the University of Illinois. B.J.L. acknowledges The American Chemical Society, Division of Medicinal Chemistry, for an ACS MEDI graduate fellowship.

Supporting Information Available: Additional information on materials and methods, including protocols for compound synthesis, NMR spectra of all new compounds, and supporting figures. This material is available free of charge via the Internet at http://pubs.acs.org.

References

(1) Jordan, M. A. Mechanism of action of antitumor drugs that interact with microtubules and tubulin. *Curr. Med. Chem.: Anti-Cancer Agents* **2002**, *2*, 1–17.
(2) Jordan, M. A.; Wilson, L. Microtubules as a target for anticancer drugs. *Nat. Rev. Cancer* **2004**, *4*, 253–265.
(3) Jordan, M. A.; Wilson, L. Microtubules and actin filaments: dynamic targets for cancer chemotherapy. *Curr. Opin. Cell Biol.* **1998**, *10*, 123–130.
(4) Giannakakou, P.; Sackett, D.; Fojo, T. Tubulin/microtubules: still a promising target for new chemotherapeutic agents. *J. Natl. Cancer Inst.* **2000**, *92*, 182–183.
(5) Mooberry, S. L.; Weiderhold, K. N.; Dakshanamurthy, S.; Hamel, E.; Banner, E. J.; Kharlamova, A.; Hempel, J.; Gupton, J. T.; Brown, M. L. Identification and characterization of a new tubulin-binding tetrasubstituted brominated pyrrole. *Mol. Pharmacol.* **2007**, *72*, 132–140.
(6) Deeken, J. F.; Loscher, W. The blood−brain barrier and cancer: transporters, treatment, and Trojan horses. *Clin. Cancer Res.* **2007**, *13*, 1663–1674.
(7) Dumontet, C.; Duran, G. E.; Steger, K. A.; Beketic-Oreskovic, L.; Sikic, B. I. Resistance mechanisms in human sarcoma mutants derived by single-step exposure to paclitaxel (Taxol). *Cancer Res.* **1996**, *56*, 1091–1097.
(8) Matesanz, R.; Barasoain, I.; Yang, C. G.; Wang, L.; Li, X.; de Ines, C.; Coderch, C.; Gago, F.; Barbero, J. J.; Andreu, J. M.; Fang, W. S.; Diaz, J. F. Optimization of taxane binding to microtubules: binding affinity dissection and incremental construction of a high-affinity analog of paclitaxel. *Chem. Biol.* **2008**, *15*, 573–585.
(9) Miller, D. S.; Bauer, B.; Hartz, A. M. S. Modulation of P-glycoprotein at the blood−brain barrier: opportunities to improve central nervous system pharmacotherapy. *Pharmacol. Rev.* **2008**, *60*, 196–209.
(10) Pellegrini, F.; Budman, D. R. Review: tubulin function, action of antitubulin drugs, and new drug development. *Cancer Invest.* **2005**, *23*, 264–273.
(11) Rice, A.; Liu, Y.; Michaelis, M. L.; Himes, R. H.; Georg, G. I.; Audus, K. L. Chemical modification of paclitaxel (Taxol) reduces P-glycoprotein interactions and increases permeation across the blood−brain barrier in vitro and in situ. *J. Med. Chem.* **2005**, *48*, 832–838.
(12) Tong, Y.-G.; Zhang, X.-W.; Geng, M.-Y.; Yue, J.-M.; Xin, X.-L.; Tian, F.; Shen, X.; Tong, L.-J.; Li, M.-H.; Zhang, C.; Li, W.-H.; Lin, L.-P.; Ding, J. Pseudolarix acid B, a new tubulin-binding agent, inhibits angiogenesis by interacting with a novel binding site on tubulin. *Mol. Pharmacol.* **2006**, *69*, 1226–1233.
(13) Mulligan, J. M.; Greene, L. M.; Cloonan, S.; Mc Gee, M. M.; Onnis, V.; Campiani, G.; Fattorusso, C.; Lawler, M.; Williams, D. C.; Zisterer, D. M. Identification of tubulin as the molecular target of proapoptotic pyrrolo-1,5-benzoxazepines. *Mol. Pharmacol.* **2006**, *70*, 60–70.
(14) Beyer, C. F.; Zhang, N.; Hernandez, R.; Vitale, D.; Lucas, J.; Nguyen, T.; Discafani, C.; Ayral-Kaloustian, S.; Gibbons, J. J. TTI-237, a novel microtubule-active compound with in vivo anti-tumor activity. *Cancer Res.* **2008**, *68*, 2292–2300.
(15) Liberatore, A.-M.; Coulomb, H.; Pons, D.; Dutruel, O.; Kasprzyk, P. G.; Carlson, M.; Nelson, A. S.; Newman, S. P.; Stengel, C.; Auvray, P.; Hesry, V.; Foll, B.; Narboux, N.; Morlais, D.; Le Moing, M.; Bernetiere, S.; Dellile, R.; Camara, J.; Ferrandis, E.; Bigg, D. C.; Prevost, G. P. IRC-083927 is a new tubulin binder that inhibits growth of human tumor cells resistant to standard tubulin-binding agents. *Mol. Cancer Ther.* **2008**, *7*, 2426–2434.

(16) Morris, P. G.; Fornier, M. N. Microtubule active agents: beyond the taxane frontier. *Clin. Cancer Res.* **2008**, *14*, 7167–7172.
(17) Dothager, R. S.; Putt, K. S.; Allen, B. J.; Leslie, B. J.; Nesterenko, V.; Hergenrother, P. J. Synthesis and identification of small molecules that potently induce apoptosis in melanoma cells through G1 cell cycle arrest. *J. Am. Chem. Soc.* **2005**, *127*, 8686–8696.
(18) Goto, H.; Tomono, Y.; Ajiro, K.; Kosako, H.; Fujita, M.; Sakurai, M.; Okawa, K.; Iwamatsu, A.; Okigaki, T.; Takahashi, T.; Inagaki, M. Identification of a novel phosphorylation site on histone H3 coupled with mitotic chromosome condensation. *J. Biol. Chem.* **1999**, *274*, 25543–25549.
(19) Bradbury, E. M. Reversible histone modification and the chromosome cell cycle. *BioEssays* **1992**, *14*, 9–16.
(20) Teicher, B. A. Newer cytotoxic agents: attacking cancer broadly. *Clin. Cancer Res.* **2008**, *14*, 1610–1617.
(21) Schwartz, G. K.; Shah, M. A. Targeting the cell cycle: a new approach to cancer therapy. *J. Clin. Oncol.* **2005**, *23*, 9408–9421.
(22) Perez de Castro, I.; de Carcer, G.; Malumbres, M. A census of mitotic cancer genes: new insights into tumor cell biology and cancer therapy. *Carcinogenesis* **2007**, *28*, 899–912.
(23) Tao, W. The mitotic checkpoint in cancer therapy. *Cell Cycle* **2005**, *4*, 1495–1499.
(24) Robinson, J.; Engelborghs, Y. Tubulin polymerization in dimethyl sulfoxide. *J. Biol. Chem.* **1982**, *257*, 5367–5371.
(25) Vichai, V.; Kirtikara, K. Sulforhodamine B colorimetric assay for cytotoxicity screening. *Nat. Protoc.* **2006**, *1*, 1112–1116.
(26) Ishiguro, K.; Ando, T.; Watanabe, O.; Goto, H. Specific reaction of [alpha],[beta]-unsaturated carbonyl compounds such as 6-shogaol with sulfhydryl groups in tubulin leading to microtubule damage. *FEBS Lett.* **2008**, *582*, 3531–3536.
(27) Watanabe, H.; Watanabe, H.; Usui, T.; Kondoh, M.; Osada, H.; Kitahara, T. Synthesis of pironetin and related analogs: studies on structure−activity relationships as tubulin assembly inhibitors. *J. Antibiot.* **2000**, *53*, 540–545.
(28) Clark, D. E.; Doherty, A. M.; Bock, M. G.; Desai, M. C.; Overington, J.; Plattner, J. J.; Stamford, A.; Wustrow, D.; Young, H. Computational Prediction of Blood−Brain Barrier Permeation. In *Annual Reports in Medicinal Chemistry*; Academic Press: New York, 2005; Vol. 40, pp 403−415.
(29) Norinder, U.; Haeberlein, M. Computational approaches to the prediction of the blood−brain distribution. *Adv. Drug Delivery Rev.* **2002**, *54*, 291–313.
(30) Ertl, P.; Rohde, B.; Selzer, P. Fast calculation of molecular polar surface area as a sum of fragment-based contributions and its application to the prediction of drug transport Properties. *J. Med. Chem.* **2000**, *43*, 3714–3717.
(31) Cruciani, G.; Pastor, M.; Guba, W. VolSurf: a new tool for the pharmacokinetic optimization of lead compounds. *Eur. J. Pharm. Sci.* **2000**, *11*, S29–S39.
(32) Kang, S.-H.; Cho, H. T.; Devi, S.; Zhang, Z.; Escuin, D.; Liang, Z.; Mao, H.; Brat, D. J.; Olson, J. J.; Simons, J. W.; LaVallee, T. M.; Giannakakou, P.; Van Meir, E. G.; Shim, H. Antitumor effect of 2-methoxyestradiol in a rat orthotopic brain tumor model. *Cancer Res.* **2006**, *66*, 11991–11997.
(33) Chamaon, K.; Stojek, J.; Kanakis, D.; Braeuninger, S.; Kirches, E.; Krause, G.; Mawrin, C.; Dietzmann, K. Micromolar concentrations of 2-methoxyestradiol kill glioma cells by an apoptotic mechanism, without destroying their microtubule cytoskeleton. *J. Neuro-Oncol.* **2005**, *72*, 11–16.
(34) Zou, H.; Zhao, S.; Zhang, J.; Lv, G.; Zhang, X.; Yu, H.; Wang, H.; Wang, L. Enhanced radiation-induced cytotoxic effect by 2-ME in glioma cells is mediated by induction of cell cycle arrest and DNA damage via activation of ATM pathways. *Brain Res.* **2007**, *1185*, 231–238.
(35) Lis, A.; Ciesielski, M. J.; Barone, T. A.; Scott, B. E.; Fenstermaker, R. A.; Plunkett, R. J. 2-Methoxyestradiol inhibits proliferation of normal and neoplastic glial cells, and induces cell death, in vitro. *Cancer Lett.* **2004**, *213*, 57–65.
(36) Kumar, A. P.; Garcia, G. E.; Orsborn, J.; Levin, V. A.; Slaga, T. J. 2-Methoxyestradiol interferes with NF{kappa}B transcriptional activity in primitive neuroectodermal brain tumors: implications for management. *Carcinogenesis* **2003**, *24*, 209–216.
(37) Tan, B.; Piwnica-Worms, D.; Ratner, L. Multidrug resistance transporters and modulation. *Curr. Opin. Oncol.* **2000**, *12*, 450–458.
(38) Gupte, A.; Mumper, R. J. Copper chelation by D-penicillamine generates reactive oxygen species that are cytotoxic to human leukemia and breast cancer cells. *Free Radical Biol. Med.* **2007**, *43*, 1271–1278.
(39) Huang, Y.; Ibrado, A. M.; Reed, J. C.; Bullock, G.; Ray, S.; Tang, C.; Bhalla, K. Co-expression of several molecular mechanisms of multidrug resistance and their significance for paclitaxel cytotoxicity in human AML HL-60 cells. *Leukemia* **1997**, *11*, 253–257.
(40) Jordan, M. A.; Kamath, K. How do microtubule-targeted drugs work? An overview. *Curr. Cancer Drug Targets* **2007**, *7*, 730–742.
(41) Ambudkar, S. V.; Kimchi-Sarfaty, C.; Sauna, Z. E.; Gottesman, M. M. P-Glycoprotein: from genomics to mechanism. *Oncogene* **2003**, *22*, 7468–7485.
(42) Alvarez, M.; Paull, K.; Monks, A.; Hose, C.; Lee, J. S.; Weinstein, J.; Grever, M.; Bates, S.; Fojo, T. Generation of a drug resistance profile by quantitation of mdr-1/P-glycoprotein in the cell lines of the National Cancer Institute Anticancer Drug Screen. *J. Clin. Invest.* **1995**, *95*, 2205–2214.
(43) Mitchison, T. J. Mitchison Lab Protocols. http://mitchison.med.harvard.edu/protocols.html.
(44) Jackman, J.; O'Connor, P. M. Methods for synchronizing cells at specific stages of the cell cycle. *Curr. Protoc. Cell Biol.* **2003**, 11–14 (Unit 8.3) .
(45) Lobert, S.; Correia, J. J. Methods for Studying Vinca Alkaloid Interactions with Tubulin. In *Microtubule Protocols*; Springer: Secaucus, NJ, 2007; pp 261−280.
(46) National Center for Biotechnology Information. http://pubchem.ncbi.nlm.nih.gov/.